

Performance evaluation of polyvinylchloride/polyacrylonitrile ultrafiltration blend membrane

Mojgan Pakbaz¹ · Zahra Maghsoud¹

Received: 13 February 2017 / Accepted: 8 October 2017 / Published online: 17 October 2017
© Iran Polymer and Petrochemical Institute 2017

Abstract Polyvinylchloride (PVC) membranes were modified by blending with polyacrylonitrile (PAN) as a second polymer. The miscibility of PVC/PAN blend was examined using an incompressible regular solution (CRS) model in no need to make a membrane. The results showed that the PVC/PAN blend was immiscible for all compositions at a temperature range of -25 to 225 °C. Furthermore, the prediction of the phase behavior of a PVC/PAN/DMF ternary system showed that the blend of two polymers was highly incompatible even in their common DMF solvent. However, this incompatibility led to a remarkable increase in the porosity of the blend membrane and pure water flux compared to those for pure PVC membrane. The pure water flux of the PVC membrane (37.9 ± 1.5 L/m² h) increased about 41 and 76% by adding 10 and 20 wt% PAN, respectively. The blend membranes also showed an enhanced flux recovery ratio (FRR) compared to a pure PVC membrane, although the PVC membrane rejection for Bovine serum albumin (BSA) was decreased after blending with PAN. The PVC/PAN (90/10) blend membrane was subjected to hydrolysis with NaOH alkaline solution at three different concentrations and contact times to further enhance its performance. The membrane, which was hydrolyzed with a 0.5 mol/L NaOH solution for 0.5 h, showed a highest pure water flux of 75.6 ± 7.2 L/m² h due to its increased hydrophilicity. This membrane also revealed an improved FRR and better thermal and mechanical properties compared to an unmodified membrane.

Keywords PVC/PAN blend membrane · Miscibility · CRS model · Hydrolysis · Modification

Introduction

The features of polyvinylchloride such as low cost, good physical and mechanical properties as well as resistance to abrasion, acid, base, and microbial corrosion are attractive for some applications, especially membrane fabrication. Polyvinylchloride has been used in the fabrication of nanofiltration and heterogeneous ion-exchange membranes [1, 2] as well as ultrafiltration [3, 4] and microfiltration [5] for wastewater treatment. Nevertheless, the hydrophobicity of PVC hampers its application in wastewater treatment due to its reduced permeation and increased fouling on the membrane surface. In fact, this drawback of PVC gives rise to hydrophobic interactions between the membrane surface and molecules of dissolved substances including proteins, resulting in protein adsorption on the membrane surface. Therefore, it reduces the efficiency of PVC membrane for filtration of aqueous solutions.

Polymer blend membranes represent an effective approach to improve the physical and chemical properties of membranes. They represent some improved membrane characteristics such as permeability, selectivity, hydrophilicity, fouling resistance, and mechanical strength [6]. Polymers such as polyvinyl butyral (PVB) [7], chlorine-modified polyvinylchloride (CPVC) [8], cellulose acetate (CA) [1], polyvinyl formal (PVF) [9], polyvinyl pyrrolidone (PVP) [10], polyethylene glycol (PEG) [11], poly(methyl methacrylate-*b*-methacrylic acid) (P(MMA-*b*-MAA)) [12], carboxylated polyvinylchloride (CPVC) [13], polyacrylonitrile (PAN) [14–16], and polycarbonate (PC) [17] have been used to modify filtration membranes based on polyvinylchloride.

✉ Zahra Maghsoud
maghsoud@um.ac.ir

¹ Chemical Engineering Department, Faculty of Engineering, Ferdowsi University of Mashhad, Mashhad, Iran

Previous studies on modification of PVC-based membranes by various polymers are summarized in Table 1.

In the given polymers, PAN is more promising for its unique characteristics such as hardness, strength, and resistance to most chemicals and solvents, originating from its polar nature. It should be noted that acrylonitrile homopolymer cannot be applied alone due to its high melting point, high melt viscosity, and poor thermal stability. Therefore, acrylonitrile is usually modified through copolymerization with other comonomers such as vinyl acetate, methyl acrylate, methyl methacrylate, vinyl chloride, etc. [18]. Due to its good chemical resistance, PAN is used in aqueous filtration processes as a membrane material [19]. In the preparation of membranes, PAN is an alternative to common polymers such as polysulfone (PS) and polyether sulfone (PES) for the features such as higher hydrophilicity, excellent solvent stability, and low price [20]. PAN has also been used as the second polymer to modify pure membranes.

Zhang et al. [21] and Amirilargani et al. [22] used PAN to modify the hydrophilicity and performance of ultrafiltration membrane using PS and PES, respectively. Gu [14] used the blend of PVC/PAN to fabricate flat ultrafiltration membranes. He investigated the miscibility of PVC/PAN blend using DSC analysis, indicating that the PVC/PAN blend was immiscible for all compositions. Thus, he used P(VC-co-AN) as a compatibilizer to enhance the membrane formation and performance. Mei et al. [15] used PVC/PAN blend for the fabrication of hollow fiber membranes. Using viscosity measurements, they found that the two polymers formed miscible blends when PAN content was in the range of 20–80 wt% PAN. They found that the immiscibility of PVC/PAN blend for PAN contents below 20 wt% or above 80 wt% led to the formation of interfacial microvoids and increased pure water flux compared to pure membranes. They also showed a maximum pure water flux for 50/50 composition, whereas no experimental data were reported for this composition. Rabiee et al. [16] also added PAN to PVC for fabrication of ultrafiltration membranes. They found that the PVC/PAN blend membrane with a blending ratio of 70/30 (PVC/PAN) exhibited the highest pure water flux and flux recovery ratio. However, the membrane pure water flux was dropped by further addition of PAN due to disappearance of finger-like pores in the membrane structure.

Another feature that makes the PAN an appropriate choice for membrane fabrication is its nitrile groups that can be simply hydrolyzed and converted to carboxyl or amide groups which are hydrophilic by nature. The hydrolysis may increase the hydrophilicity and surface charge of polyacrylonitrile membrane, improving the performance of membrane and fouling resistance. Inherent properties of polyacrylonitrile membrane (structure and surface properties) indicate that hydrolysis can affect the membrane surface in terms of hydrophilicity and pore size

[23]. Reddy and Patel [24] modified a PES/PAN ultrafiltration blend membrane using an alkaline solution at different concentrations at ambient temperature for 24 h. According to their results, the modified membranes exhibited greater recovery flux compared to the non-modified membrane due to the increase in hydrophilicity. Zhang et al. [21] hydrolyzed a PSf/PAN blend membrane using 8% NaOH solution at 75 °C for 1 h. Their results demonstrated an increase in the pore size and pure water flux passing through the membrane. In addition, the recovery ratio of water flux increased from 49.2 to 79.5% by hydrolysis reaction. Mei et al. [25] also modified a PVC/PAN/SiO₂ composite hollow fiber blend membrane using a NaOH solution of varying concentrations at 80 °C for 70 min. Their results revealed greater water flux and anti-fouling properties of hydrolyzed membranes due to enhanced hydrophilicity. They reported that hydrolysis reaction was only observed on the membrane surface and interfacial microvoids grew larger at low concentrations of NaOH. However, with an increase in NaOH concentration, both membrane surface and body were hydrolyzed and interfacial microvoids disappeared only to be converted into micropores. In the previous studies, a decrease in the pore size of PAN ultrafiltration membranes caused by high concentrations and prolonged hydrolysis times was also reported [20, 26, 27].

Although immiscible polymer blends could form membranes with enhanced pure water flux, the high incompatibility between the blend components might suppress the formation of a homogenous film. Therefore, the phase behavior of the polymer blend plays a crucial role in controlling the membrane structure and performance. In this study, we focused on PVC/PAN blend membranes, for which the disparity between phase behaviors has been reported [14–16]. Here, the miscibility of PVC/PAN blend was examined using a simple thermodynamic theory based on the compressible regular solution (CRS) model and viscosity measurements. Then, the blend membrane characteristics and performances were evaluated using Fourier transform infrared spectroscopy (FTIR), scanning electron microscopy (SEM), thermogravimetric analysis (TGA), contact angle, surface roughness, porosity, pure water flux, and rejection measurements. Furthermore, to modify the prepared membranes, the PVC/PAN (90/10) blend membrane was selected and hydrolyzed using an alkaline solution of NaOH at a constant temperature of 70 °C. As far as we know, the previous studies have only considered the hydrolysis of PAN at a constant concentration with varying modification time, or at a given specific time with varying concentration. In this study, however, we conducted the hydrolysis tests at three different concentrations and at different time periods to determine the proper hydrolysis condition.

Table 1 Summary of the previous studies of modification of PVC-based membranes with different polymers

References	Polymers used for modification of PVC membranes	Type of membrane/separation process	Results
Gholami et al. [1]	(CA)	Nanocomposite nanofiltration membrane	Increase in pure water flux by increasing CA content from 2.5 to 10 wt% due to increase in hydrophilicity
Peng and Siu [7]	(PVB)	Flat sheet membrane/ultrafiltration	Increase in pure water flux from 7.8 to 394.7 L/m ² h by increasing PVB content from 0 to 10 wt% due to increase in hydrophilicity. Reduction of the pure water flux by further increase of PVB content over 10 wt% due to morphological changes
Liu et al. [8]	(CPVC)	Flat sheet membrane/ultrafiltration	Increase in pure water flux from 142.5 to 292.3 L/m ² h by increase in CPVC content from 0 to 100 wt% due to increase in membrane hydrophilicity. (20 wt% Pluronic F127 was used as pore forming agent)
Fan et al. [9]	(PVF)	Flat sheet membrane/ultrafiltration	Increasing pure water flux from 52.1 to 323.6 L/m ² h by increase in PVF content from 2 to 8 wt% due to increase in membrane hydrophilicity, pore size and porosity
Babu and Gaikar [10]	(PVP)	Flat sheet membrane/ultrafiltration	Increase in pure water flux from 174.1 to 645.5 L/m ² h with increase in PVP content from 0 to 2 wt % at a constant concentration of PVC (11 wt %).
Davood Abadi Farahani [11]	(PEG)	Flat sheet membrane/ultrafiltration	Increase of the membrane pure water flux from 125 to 166 kg/m ² h by increasing PEG content from 0 to 6 wt% for 13 wt% PVC in casting solution, due to increase in hydrophilicity and porosity. Reduction of the membrane pure water flux from 183 to 120 kg/m ² h by increasing PEG content from 0 to 6 wt% for 15 wt% PVC in the casting solution due to higher solution viscosity and hence formation of a dense top layer
Liu et al. [12]	(P(MMA- <i>b</i> -MAA))	Flat sheet membrane	P(MMA- <i>b</i> -MAA) induced proper hydrophilic properties in the membrane. With increase of PMAA arm length, the pure water flux, foulant solution permeability and water flux recovery of the blend membranes enhanced
Babu and Gaikar [13]	(CPVC)	Flat sheet membrane/ultrafiltration	Increasing the membrane pure water flux from 156.54 to 207.68 L/m ² h by increase in CPVC content from 0 to 10 wt% due to higher membrane porosity. Reduction of pure water flux by increasing CPVC content by above 10 wt% due to enhanced intermolecular interactions
Gu [14]	(PAN)	Flat sheet membrane/ultrafiltration	The pure water flux of the membrane increased from 493 to 554 L/m ² h by changing the PVC/PAN ratio from 9 to 4 due to higher immiscibility between PVC and PAN

Table 1 (continued)

References	Polymers used for modification of PVC membranes	Type of membrane/separation process	Results
Mei et al. [15]	(PAN)	Hollow fiber membrane	The pure water flux and porosity of PVC/PAN blend membrane were better than pure PVC membrane due to the enhanced membrane hydrophilicity and formation of interfacial microvoids by adding PAN to PVC, because of the immiscibility of PVC/PAN blend
Rabiee et al. [16]	(PAN)	Flat sheet membrane/ultrafiltration	The pure water flux increased from 213 kg/m ² h (pure PVC membrane) to 343 kg/m ² h (70/30: PVC/PAN membrane) due to higher hydrophilicity and change in membrane morphology caused by addition of PAN to PVC
Pacharasakoolchai and Chinpa [17]	(PC)	Flat sheet membrane/ultrafiltration	Increase in pure water flux and reduction of rejection by increasing PC content beyond 1.5 wt% due to the immiscibility of PVC and PC. The blend membrane with 0.75 wt% PC had higher water flux and mechanical strength compared to pure PVC membrane

* All flux measurements were carried out under a transmembrane pressure of 100 kPa, except for Refs. [7] (200 kPa) and [11] and [16] (300 kPa)

Experimental

Materials

PVC (S70) was purchased from Bandar Imam Petrochemicals Co., Iran. PAN consisted of 92% acrylonitrile (by weight) and 8% vinyl acetate as the comonomer, with an average molecular weight of 75000 g/mol, was kindly provided by Polyacryl Co., Iran. *N,N*-Dimethylformamide (DMF) (Merck, Germany) and distilled water were used as a solvent and non-solvent, respectively. Bovine serum albumin (BSA, M_w 66 kDa) (Sigma Aldrich, Canada) was used for the evaluation of rejection and anti-fouling properties of the membranes. Sodium hydroxide (Dr. Mojallali, Iran) was adopted for the hydrolysis reaction.

Membrane preparation

PVC/PAN blend membranes were prepared by phase inversion method. For this purpose, PVC/PAN blend solutions containing 12 wt% total polymer were prepared with various PAN contents (0, 10, 20, 30, 40, 50, 60, 70, 80, 90, and 100). However, as discussed in the following sections, the membranes could not be fabricated from PVC/PAN blends containing more than 20 wt% PAN and pure PAN. To obtain homogeneous solutions, they were stirred for 48 h at 65 °C and an ultrasonic bath was used for 30 min

to remove entrapped air bubbles. The solutions were cast on a glass plate with a thickness of 200 μm and immersed immediately into a bath of distilled water. For complete removal of the solvent, the membranes were placed in a freshwater bath for 24 h.

Modification of membranes

To modify the blend membrane, the PVC/PAN blend 90/10 membrane was selected and hydrolyzed at different concentrations of NaOH (0.5, 1, and 1.5 M) at three different time periods (0.5, 1, and 1.5 h) and at a constant temperature (70 °C). After hydrolysis, the membranes were washed with sufficient water to neutralize the unreacted NaOH.

Characterization

Scanning electron microscopy (SEM)

The surface and cross-sectional morphology of the membranes were examined using scanning electron microscopy (LEO1450VP model, Zei Co., Germany). The membranes were frozen and then broken in liquid nitrogen and finally coated with gold–palladium.

Water contact angle

The contact angle of water and membranes surfaces was measured using an optical microscope (OlympusSZH10, Japan) to investigate the hydrophilicity of the membranes. The mean contact angle of each specimen was measured at three locations on each sample.

FTIR spectroscopy

Fourier transform infrared spectroscopy is a useful way to identify different functional groups present in polymers and to characterize the changes in the chemical structure of a membrane surface during modification by chemical agents such as NaOH. Fourier transform infrared spectrometer (FTIR Avatar 370 Nicolet Spectrometer, USA) was used to investigate the chemical structure of the membranes.

Atomic force microscopy

Atomic force microscopy (AFM) was performed with an AFM (Full model, Ara research Co., Iran) to evaluate the membrane surface roughness. The surface roughness was reported in terms of the root mean square (RMS) roughness based on the scan size of $5 \times 5 \mu\text{m}^2$. Image acquisition and processing were performed by an Imager software (Version 1.00 Ara Research CO).

Thermogravimetric analysis

Thermal stability of the membranes was studied using a TGA device (TGA-50 model, Shimadzu Co, Japan). In this experiment, the membrane samples were heated at a constant rate of $10 \text{ }^\circ\text{C}/\text{min}$ from 25 to $800 \text{ }^\circ\text{C}$ and their weight loss was recorded.

Evaluation of mechanical strength

To evaluate the mechanical properties of fabricated membranes, a tensile test machine (Zwick Z250, Germany) was used. For this test, samples were cut into pieces with a width of 70 mm and a length of 10 mm. Each membrane was then held at a distance of 1 cm from the edge and placed in the machine. The crosshead velocity was assumed to be 5 mm/min.

Membrane porosity

Membrane porosity was calculated based on the weights of wet and dry membranes. Each membrane was placed in distilled water for 24 h, and after removing the excess water from the surface, the weight of the wet membrane was measured. The weight of the dry membrane was measured

after being dried at ambient temperature. The porosity of the membrane was measured using the Eq. 1 as follows [9]:

$$\varepsilon(\%) = \frac{W_w - W_d}{\rho_w A \delta_0} \times 100, \quad (1)$$

where $\varepsilon(\%)$ is the porosity of membrane, W_w (g) and W_d (g) represent the weight of wet and dry samples, respectively, ρ_w (g/cm^3) is the density of pure water, and A (cm^2) and δ_0 (vm) are the area and thickness of wet membranes, respectively.

Evaluation of pure water flux, rejection, and pure water flux recovery ratio (FRR)

A cross-flow test cell was used to measure the pure water flux. All measurements were carried out at ambient temperature at 100 kPa pressure. The membranes were compressed under a pressure of 150 kPa for half an hour to stabilize the measurement conditions, and then, the pressure was reduced to the operating pressure (100 kPa). The pure water flux value was calculated using the Eq. 2 as follows [8, 9]:

$$J_w = \frac{V}{A \Delta t}, \quad (2)$$

where J_w ($\text{L}/\text{m}^2 \text{ h}$) is the pure water flux, V (L) is the volume of water passing through the membrane, A (m^2) is the effective area of the membrane, and Δt (h) is the permeation time.

In the next step, the rejection (r) of membranes was measured with 0.5 g/L of BSA. The rejection of BSA was calculated from the following equation [8, 9]:

$$r = \left(1 - \frac{C_p}{C_f}\right) \times 100, \quad (3)$$

where C_p and C_f (g/L) are the BSA concentrations in the permeate and feed solutions, respectively. The concentration of BSA was measured by a UV spectrophotometer (CECIL SERIES 9000, United Kingdom) at a wavelength of 278 nm [9, 14].

To study the anti-fouling properties of membranes, the recovery ratio of pure water flux was measured. After measuring the rejection of BSA, membrane was washed with distilled water at a pressure of 2 bar for 20 min. The pure water flux of the washed membrane was measured again until it became steady. The recovery ratio of pure water flux of the membrane was calculated using the following equation [8]:

$$\text{FRR} = \frac{J_{w2}}{J_{w1}} \times 100\%, \quad (4)$$

where FRR, J_{w1} , and J_{w2} are the flux recovery ratio and pure water flux of membrane before and after washing, respectively.

Dilute solution viscometry (DSV)

The study of the intrinsic viscosity of a ternary system including two polymers and a solvent has attracted growing attention due to the simplicity and reliability of investigating the intermolecular interactions between two different polymers in a solvent. According to the dilute solution viscometry (DSV) method, the attractive interaction between the chains of two polymers in a solution leads to the expansion of polymer coils and augmentation of intrinsic viscosity. This intrinsic viscosity is larger than the value computed by the additivity law, with the reverse applying to repulsive interactions [28].

The compatibility of PVC/PAN blend was investigated using DSV method. Viscosity measurements were performed using an Ubbelohde viscometer (Fisher Scientific Co., Germany) at 27 ± 0.1 °C. For this purpose, the dilute solutions ($C < C^*$) of PVC/PAN blend were prepared in DMF (0, 20, 40, 60, 80, and 100 wt% of PAN). The compatibility of PVC/PAN blend was evaluated according to the following equation [28]:

$$\Delta[\eta] = [\eta]_{\text{exp}} - [\eta]_{\text{cal}}, \quad (5)$$

where $[\eta]_{\text{exp}}$ and $[\eta]_{\text{cal}}$ are the experimental and calculated intrinsic viscosities (mL/g), respectively. $[\eta]_{\text{cal}}$ was calculated based on the additivity law (Eq. 6) [15, 28]:

$$[\eta]_{\text{cal}} = [\eta]_1 w_1 + [\eta]_2 w_2, \quad (6)$$

where $[\eta]_i$ and w_i are the intrinsic viscosity and weight fraction of component i in the blend solution, respectively. The intrinsic viscosities were calculated by extrapolation to zero concentration (c) according to the following equations [15, 29]:

$$\frac{\eta_{\text{sp}}}{c} = [\eta] + K_H [\eta]^2 c, \quad (7)$$

$$\frac{\ln \eta_{\text{rel}}}{c} = [\eta] + K_K [\eta]^2 c, \quad (8)$$

where K_H and K_K are the Huggins and Kraemer constants, respectively. η_{sp} (specific viscosity) and η_{rel} (relative viscosities) were calculated using the following equations [15]:

$$\eta_{\text{sp}} = \eta_{\text{rel}} - 1, \quad (9)$$

$$\eta_{\text{rel}} = \frac{t}{t_0}, \quad (10)$$

where t and t_0 are the pour times of polymer solution and pure solvent in the Ubbelohde viscometer, respectively.

Theoretical background of the compressible regular solution (CRS) model

The compressible regular solution (CRS) model is a simple theory for calculation of the free energy of mixing of weakly interacting polymer blends. The compressibility is regarded in this model through the reduced density parameter. Furthermore, this model is merely dependent on pure component properties such as mass density, solubility parameter, and thermal expansion coefficient, which are available in the literature or can be calculated or simulated in a simple way [30]. The Gibbs free energy of mixing per unit volume of a binary polymer blend at atmospheric pressure based on the CRS model is as follows [30]:

$$\begin{aligned} \Delta g_{\text{mix}} = kT & \left[\frac{\phi_A \tilde{\rho}_A}{N_A \nu_A} \ln \phi_A + \frac{\phi_B \tilde{\rho}_B}{N_B \nu_B} \ln \phi_B \right] \\ & + \phi_A \phi_B \tilde{\rho}_A \tilde{\rho}_B (\delta_{A,0} - \delta_{B,0})^2 \\ & + \phi_A \phi_B (\tilde{\rho}_A - \tilde{\rho}_B) (\delta_A^2 - \delta_B^2), \end{aligned} \quad (11)$$

where ϕ_i is the volume fraction of polymer, N_i is the degree of polymerization, k is the Boltzmann constant, T is the absolute temperature, $\nu_i = M_{\text{ui}} / (N_{\text{av}} \rho \times i)$ is the hard core (0 K, zero pressure) segment volume, in which M_{ui} is the molecular weight of the repeat unit, N_{av} is the Avogadro's number, and $\rho \times i$ is the hard core density. δ_i is the solubility parameter at temperature T , which can be calculated by $\delta_i^2 = \tilde{\rho}_i \delta_{i,0}^2$, where $\delta_{i,0}$ is the hard core density of component i and is calculated using the relationship $\delta_i^2(T) = \delta_i^2(298) ((\tilde{\rho}_i(T)) / (\tilde{\rho}_i(298)))$ at $T = 0$ K. In addition, $\delta_i(298)$ is the solubility parameter of components at 298 K. The reduced density is defined as $\tilde{\rho}_i = \rho_i / \rho \times i$, where $\rho_i = \rho \times i \exp(-\alpha_i T)$ is the mass density and α_i is the thermal expansion coefficient. The parameters required to plot the Δg_{mix} curve for the PVC/PAN blend are shown in Table 2.

Here, to predict the phase behavior of the ternary PVC/PAN/DMF system, the spinodal curve was plotted. For a

Table 2 Parameters required to plot the curve

Component	α (10^{-4} K^{-1})	δ (298 K) (MPa) ^{1/2}	ρ_i (g/cm ³)	ν ($10^{-23} \text{ cm}^3/\text{mol}$)
PVC ^a	7.4	19.9	1.79	5.798
PAN ^b	2.518	26.508	1.264	7.318
DMF ^c	10.43	24.8	1.289	12.74

^a P–V–T data from Ref. [30] and solubility parameter at $T = 298$ °C from Ref. [31]

^b P–V–T data from Ref. [32]

^c P–V–T data from Ref. [33] and solubility parameter at $T = 298$ °C from Ref. [34]

ternary system, the Gibbs free energy of mixing is calculated as follows:

$$\begin{aligned} \Delta g_{\text{mix}} = kT & \left[\frac{\phi_1 \tilde{\rho}_1}{N_1 v_1} \ln \phi_1 + \frac{\phi_2 \tilde{\rho}_2}{N_2 v_2} \ln \phi_2 + \frac{\phi_3 \tilde{\rho}_3}{N_3 v_3} \ln \phi_3 \right] + \phi_1 \phi_2 \tilde{\rho}_1 \tilde{\rho}_2 (\delta_{1,0} - \delta_{1,0})^2 \\ & + \phi_1 \phi_2 (\tilde{\rho}_1 - \tilde{\rho}_2) (\delta_1^2 - \delta_2^2) + \phi_1 \phi_3 \tilde{\rho}_1 \tilde{\rho}_3 (\delta_{1,0} - \delta_{3,0})^2 \\ & + \phi_1 \phi_3 (\tilde{\rho}_1 - \tilde{\rho}_3) (\delta_1^2 - \delta_3^2) + \phi_2 \phi_3 \tilde{\rho}_2 \tilde{\rho}_3 (\delta_{2,0} - \delta_{3,0})^2 \\ & + \phi_2 \phi_3 (\tilde{\rho}_2 - \tilde{\rho}_3) (\delta_2^2 - \delta_3^2). \end{aligned} \quad (12)$$

The spinodal was calculated using the material balance equation ($\phi_1 + \phi_2 + \phi_3 = 1$) and the following equations [35]:

$$G_{22}G_{33} = (G_{23})^2, \quad (13)$$

$$G_{ij} = \left(\frac{\partial^2 \overline{\Delta G_M}}{\partial \phi_i \partial \phi_j} \right)_{v_{\text{ref}}}, \quad (14)$$

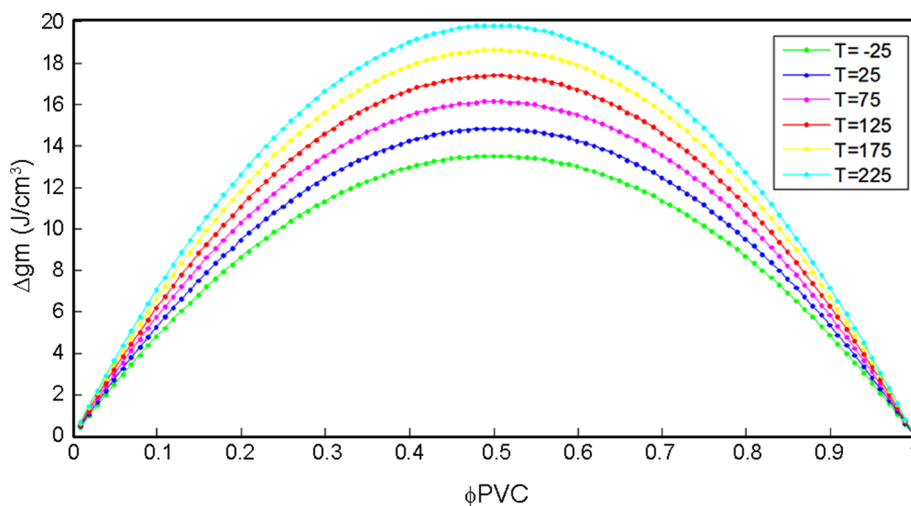
where $\overline{\Delta G_M}$ is the Gibbs free energy of mixing on a unit volume basis and v_{ref} is the molar volume of the reference component (the molar volume of component 1) [35]. Thus, G_{ij} was calculated as the following equations:

$$G_{22} = \frac{1}{\phi_1} + \frac{V_1}{V_2 \phi_2} - 2 \frac{(\tilde{\rho}_1 \delta_{1,0} - \tilde{\rho}_2 \delta_{2,0})^2}{RT} V_1, \quad (15)$$

$$\begin{aligned} G_{23} = \frac{1}{\phi_1} & - \left[\frac{(\tilde{\rho}_1 \delta_{1,0} - \tilde{\rho}_2 \delta_{2,0})^2}{RT} + \frac{(\tilde{\rho}_1 \delta_{1,0} - \tilde{\rho}_3 \delta_{3,0})^2}{RT} \right] V_1 \\ & + \left(\frac{V_1}{V_2} \right) \frac{(\tilde{\rho}_2 \delta_{2,0} - \tilde{\rho}_3 \delta_{3,0})^2}{RT} V_2, \end{aligned} \quad (16)$$

$$G_{33} = \frac{1}{\phi_1} + \left(\frac{1}{\phi_3} \right) \left(\frac{V_1}{V_3} \right) - 2 \frac{(\tilde{\rho}_1 \delta_{1,0} - \tilde{\rho}_3 \delta_{3,0})^2}{RT} V_1, \quad (17)$$

Fig. 1 Curves for PVC/PAN blend as a function of PVC volume fraction at different temperatures (°C)



where V_i is the molar volume of pure components, achieved from the following equation:

$$V_i = \frac{N_i v_i}{\tilde{\rho}_i}. \quad (18)$$

Since the PAN used here was a copolymer of acrylonitrile (92%) and vinyl acetate (8%), its solubility parameter was calculated based on the mixture rule as follows [36]:

$$\delta_{\text{P(AN-CO-VAc)}} = \delta_{\text{PAN}} x_{\text{PAN}} + \delta_{\text{PVAc}} x_{\text{PVAc}}, \quad (19)$$

where δ_{PAN} and δ_{PVAc} are the solubility parameters of PAN and PVAc [31], respectively, and x_i is the weight percent of monomer i in the copolymer.

Results and discussion

Miscibility of PVC/PAN blend based on the CRS model

The curves of Δg_{mix} were plotted for the PVC/PAN blend in terms of volume fraction of PVC in the temperature range of -25 to 225 °C (Fig. 1). The negative value of Δg_{mix} is an insufficient but necessary requirement for a miscible polymer blend [31]. As shown in Fig. 1, the PVC/PAN blend is immiscible in the given temperature range, since Δg_{mix} is positive for all compositions. As far as we know, the phase behavior of the PVC/PAN blend with temperature has not

been explored in the previous studies [14–16]. However, the formation of interfacial microvoids, and hence, a higher porosity and improved performance of their blend membranes have been attributed to the immiscibility of the two polymers [15].

The combinatorial mixing entropy of polymer blends is usually negligible owing to the high molecular weight of polymer blend components. Therefore, a negative mixing enthalpy is required to induce miscibility. This can be obtained through strong specific interactions of blend components. In the absence of these interactions, the miscibility is dependent on temperature, composition, and additives such as compatibilizers or solvents [37]. Therefore, in this paper, the effect of solvent on the miscibility of PVC/PAN blend was investigated using the CRS ternary model in the following sections.

Phase behavior prediction of PVC/PAN blend in DMF (solvent)

The ternary spinodal curve of PVC/PAN/DMF system was plotted using Eqs. 12–17, as shown in Fig. 2. As can be seen, miscibility is not attained unless the solvent content in the polymer solution is above ~ 99.4%, where the combinatorial entropy due to the presence of small molecules dominates the free energy. Therefore, PVC and PAN may form an immiscible blend even in a common solvent like DMF. It was observed that all PVC/PAN blend solutions containing 12 wt% total polymer with different ratios were opaque (Fig. 2), which confirmed the incompatibility of PVC/PAN blend in DMF, as shown with the CRS ternary model. However, the polymer solution containing 0.5 wt% of the total polymer (99.5 wt% solvent) was transparent, which implies that the PVC/PAN blend is miscible in this case.

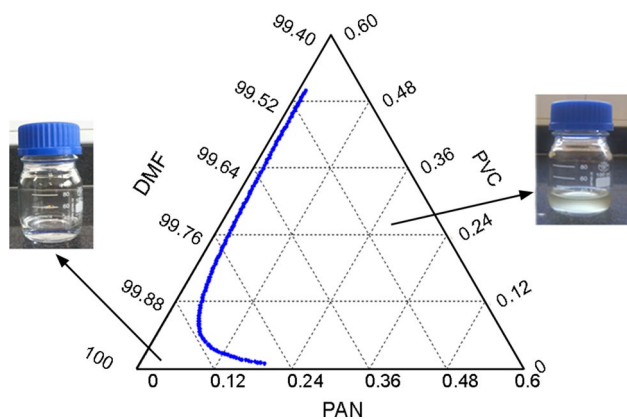


Fig. 2 Ternary spinodal curve of PVC/PAN/DMF at $T = 25$ °C, as well as transparent and opaque solutions made with total polymer concentrations of 0.5 (left) and 12 wt% (right)

Compatibility study of PVC/PAN blend using DSV method

Figure 3 shows the $\Delta[\eta]$ values obtained from Eq. 5 for the PVC/PAN blend solutions with different PAN contents in DMF at 27 °C. As can be seen, the $\Delta[\eta]$ values for the blend of PVC and PAN are non-zero due to deviation from the additivity law. A positive deviation is observable at $W_{\text{PAN}} > 0.2$, which shows the expansion of PVC and PAN coils, possibly due to their increased compatibility, and the negative deviation is evident at $W_{\text{PAN}} \leq 0.2$, meaning that the shrinking of PAN and PVC coils is caused by their incompatibility. According to these results, the DSV method showed miscibility or compatibility for higher values of PAN in the polymer blend (> 20 wt%), which could be an indication of the increased inherent tendency between two polymers caused by specific interactions between polymer segments.

According to the results of CRS model (Fig. 1), Δg_{mix} values rise with an increase in temperature, which confirms the existence of some favorable enthalpic interactions that disappear at higher temperatures. However, these interactions are weak, because no LCST behavior was observed for the PVC/PAN blend. Moreover, the comparison of the results of CRS model and DSV method revealed the discrepancies in determining the miscibility range of the PVC/PAN blend. As discussed earlier, the CRS model predicted complete immiscibility for the whole range of blend composition, while the DSV method showed positive $\Delta[\eta]$ values for PAN contents beyond 20 wt%, which was an indication of the miscibility or compatibility of these compositions. It should be noted that the DSV method is based on dilute polymer solutions, where according to the ternary phase diagram, miscibility is expected at infinite dilution and a clear solution is observed experimentally (Fig. 2). However, when it comes to higher concentrations, thermodynamic instability increases and phase separation occurs, irrespective of the blend composition. On the other hand, the high molecular weight of the

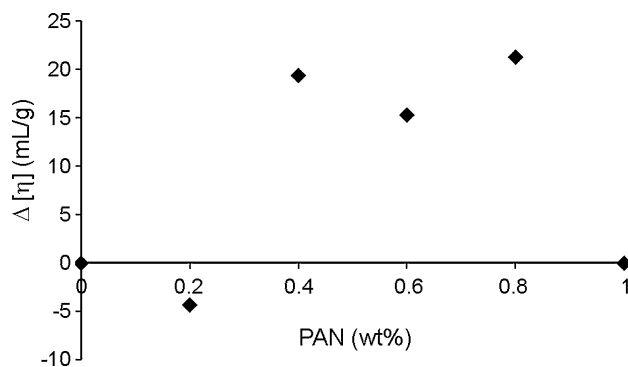


Fig. 3 Variation of PAN content (wt%) in PVC/PAN blend

blend components results in negligible entropy of mixing, though this term is not accounted for in the DSV method. Therefore, it seems that the CRS model gives a more complete description of the system thermodynamics.

Membrane formation from PVC/PAN blend with different ratios

During the preparation of PVC/PAN blend solutions in DMF with different ratios, it was observed that membranes could not be obtained from PVC/PAN blends containing more than 20 wt% PAN. For compositions containing up to 40 wt% PAN, the cast solution was instantly converted to a heterogeneous film at the time of immersion into the coagulation bath. This was ascribed to the high incompatibility of PVC and PAN, which was intensified by immersion into the non-solvent bath. In addition, membranes could not be formed by increasing the PAN content beyond 40 wt%, despite the formation of a homogeneous film, which was due to the lack of sufficient mechanical strength. Similarly, fabricated membranes from pure PAN lacked the proper strength required for a membrane. Therefore, it appeared that for higher values of PAN in the PVC/PAN blend membrane (≥ 40 wt%), PVC represented the dispersed phase in the PAN matrix, and hence, the membranes were not be attainable due to the absence of appropriate mechanical properties. According to the above points, in this study, the composition of PVC/PAN blend membranes was limited to 20 wt% PAN. Therefore, in the following sections, membrane characteristics are only reported for these compositions.

Gu [14] has made similar observations about problematic membrane formation from PVC and PAN, using a compatibilizer to improve their compatibility and mechanical properties. However, in the study of Mei et al. [15], the blend membrane was reported for all compositions of PVC and PAN, despite the fact that they were reported as incompatible for PAN contents out of 20–80 wt% range.

Contact angle and porosity of PVC/PAN blend membranes

Figure 4 shows the contact angle and porosity of PVC/PAN blend membranes. It can be seen that the contact angle of pure PVC membrane drops by adding 20 wt% PAN from $71.9^\circ \pm 0.7^\circ$ to $64.4^\circ \pm 5^\circ$. This reduction of contact angle by adding PAN to PVC corresponds to improved hydrophilicity of PVC membrane. The overall porosity of pure PVC membrane is $6.5 \pm 3.3\%$. However, the membrane porosity increases to $63.7 \pm 4.2\%$ by adding 20 wt% PAN to PVC. The immiscibility of PVC/PAN blend is a major cause of substantial increase in the membrane porosity, achieved by adding PAN to PVC.

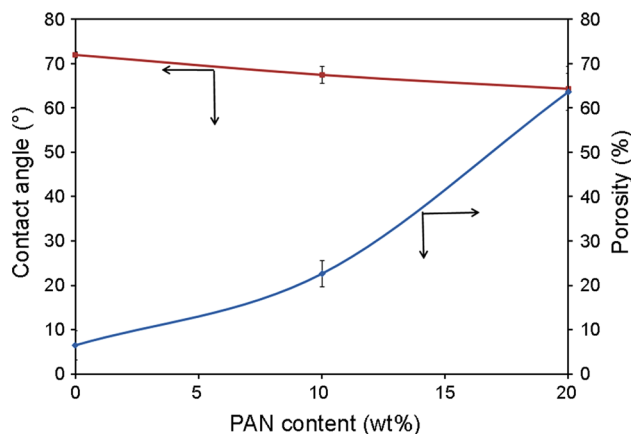


Fig. 4 Contact angle and porosity of PVC/PAN blend membranes

During the phase inversion process, two rich and dilute phases were formed. In addition to the polymer–liquid demixing, the separation of polymer–polymer phase occurred as a result of different interactions of polymer blend components with solvent. When two polymers are immiscible, the intensity of polymer–polymer phase separation in the rich phase is increased; resulting in the formation of interfacial microvoids, and thus, the membrane porosity is enhanced. Hydrophilicity of PAN is another reason for the improvement of blend membrane porosity. Consequently, during the first moments of membrane formation, the hydrophilicity of PAN stimulated the diffusion of water into the sublayer, leading to the formation of more pores and increased overall porosity [9].

Morphology and surface roughness of PVC/PAN blend membranes

SEM micrographs of the surface and cross section of the PVC/PAN blend membranes are shown in Fig. 5. As shown in Fig. 5a, the surface pores in pure PVC membrane are not obvious, but the surface of PVC/PAN blend membranes has some pores (Fig. 5b, c), which might be due to the high immiscibility of PVC/PAN blend. Moreover, the number and size of surface pores rise with an increase in PAN content from 10 to 20 wt%. The cross-sectional morphology of pure PVC and PVC/PAN (90/10) blend membranes is an asymmetric structure consisting of a top layer and a porous sublayer (Fig. 5d, e). The cross section of pure PVC membrane exhibits a sublayer of a finger-like structure with a sponge-like structure at the bottom. However, by adding 10 wt% PAN to PVC, the finger-like pores are grown further and the morphology of bottom surface changes from sponge-like to the macropores (Fig. 5e). This might be due to the fact that the solidification of the polymer-rich phase is delayed by adding PAN to PVC, and hence, the finger-like pores grow

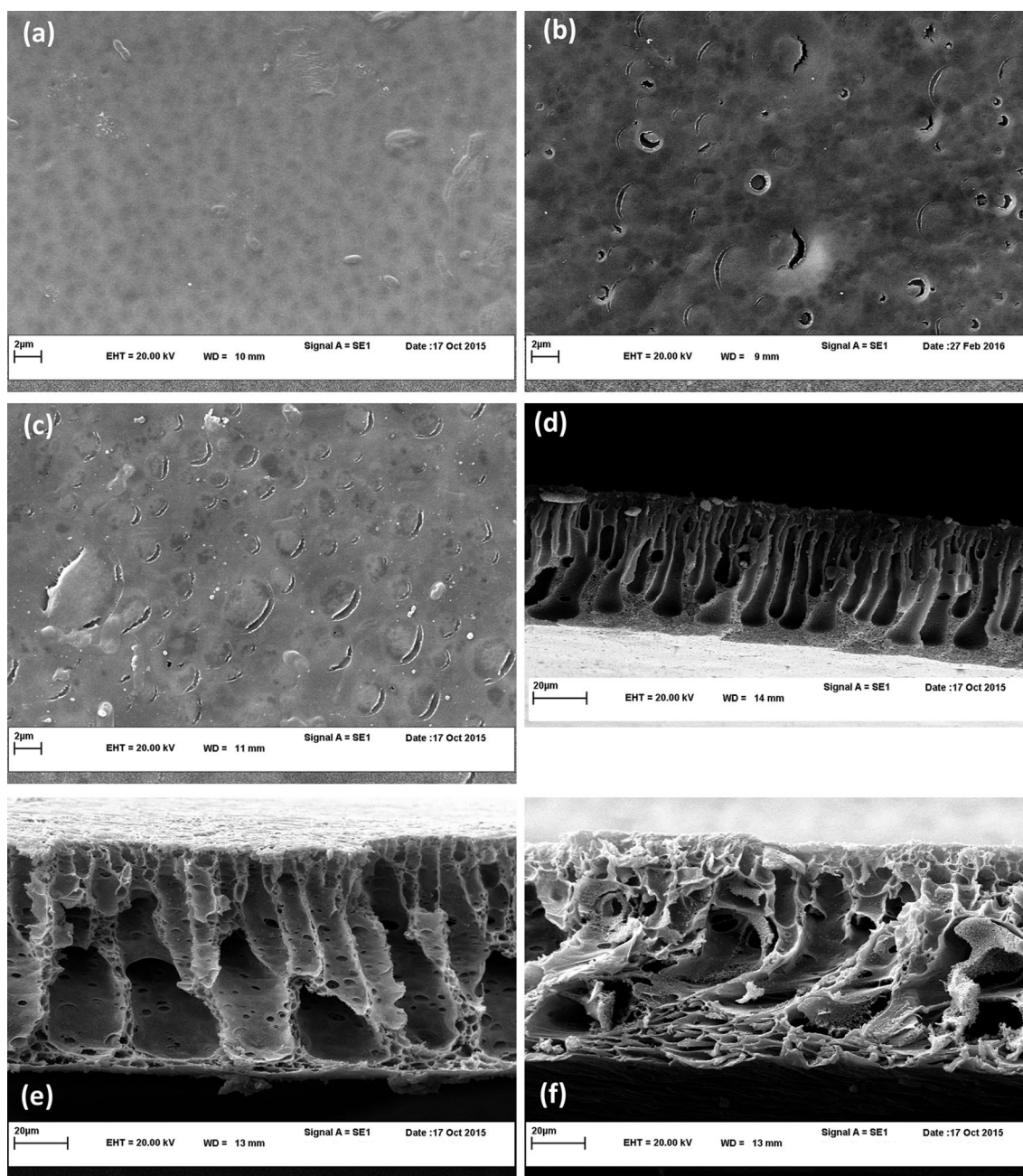


Fig. 5 SEM micrographs of the surface (left) and cross-section (right) of PVC/PAN blend membranes with different PAN contents in the PVC/PAN blend **a** and **d** 0 wt%; **b** and **e** 10 wt%; **c** and **f** 20 wt%

further. Furthermore, during membrane formation, the weak interaction of PVC/PAN blend creates larger gaps between PVC and PAN in the rich phase. The rapid movement of solvent and non-solvent through these gaps may lead to the formation of finger-like macrovoids. When the content of PAN in the PVC/PAN blend membrane is increased to 20 wt%, the structure of pores collapses and an irregular structure is formed (Fig. 5f). The formation of this structure may be due to the immiscibility intensity of PVC/PAN blend caused by

increasing the PAN content. As mentioned earlier, further increase of PAN content (> 20 wt%) led to the formation of highly heterogeneous films, which could not be used as membranes.

As shown in Table 3, the RMS roughness of pure PVC membrane increases from 1.93 ± 0.42 to 9.18 ± 2 nm by adding 20 wt% PAN. This increased surface roughness caused by the addition of PAN to PVC could be attributed to the formation of larger pores on the membrane surface

Table 3 Separation performance, mechanical properties, and root mean square (RMS) roughness of membranes

Membranes	Pure water flux (L/m ² h)	Rejection (%)	FRR (%)	Elongation (%)	Tensile strength (MPa)	RMS roughness (nm)
Pure PVC	37.9 ± 1.5	98.8 ± 1.7	45.6	43.6	3.5	1.93 ± 0.42
PVC/PAN (90/10)	53.5 ± 5.1	94 ± 0.7	57.6	45.3	1.9	5.4 ± 1.42
PVC/PAN (80/20)	66.7 ± 5.8	91.4 ± 4.2	57.8	50.2	1.7	9.18 ± 2
Hydrolyzed PVC/PAN (90/10)*	75.6 ± 7.2	92.4 ± 3.8	71.6	52.2	2.6	10.1 ± 1.96

* Hydrolyzed at a concentration of 0.5 mol/L and modification time of 0.5 h

(Fig. 5) and increased membrane porosity, as shown in Fig. 4. Panda and De [38] also indicated increased surface roughness due to the larger pore size and membrane porosity induced by the addition of polyurethane to PAN.

Performance of PVC/PAN blend membranes

Table 3 shows pure water flux and rejection of PVC/PAN blend membranes. As can be seen, the PVC/PAN blend membranes have higher pure water flux and lower rejection compared to the pure PVC membrane. The pure water flux of the PVC membrane is 37.9 ± 1.5 L/m² h, while its values for the PVC/PAN blend membranes containing 10 and 20 wt% PAN are 53.5 ± 5.1 and 66.7 ± 5.8 L/m² h, respectively. One reason for the enhanced pure water flux is the greater hydrophilicity of PAN compared to PVC. The formation of interfacial microvoids due to the immiscibility of PVC/PAN blend is another reason for improvement of the blend membrane pure water flux [15, 21]. The BSA rejection of pure PVC membrane was reduced by adding 20 wt% PAN to PVC from 98.8 ± 1.7 to 91.4 ± 4.2. Since the dependence of rejection on the morphology of membrane surface is greater than that on the structure of the cross section [39], this reduction in the rejection probably accounts for the change in the membrane surface morphology caused by adding PAN to PVC as revealed by SEM analysis.

Effect of PAN on membrane anti-fouling properties

Figure 6 presents the FRR values of membranes. As can be seen, the values of FRR in both 90/10 and 80/20 PVC/PAN blend membranes are higher than that of PVC membrane. It can be noted that the addition of PAN to PVC increases the membrane hydrophilicity and surface roughness, which the hydrophilicity is responsible for a lower interaction between the membrane surface and foulant. This results in more convenient washing of the membrane surface and hence the higher pure water flux recovery of the membranes. It has been shown that increasing the surface roughness makes the membranes especially prone to fouling [40], but the higher FRR values with increased surface roughness have also been

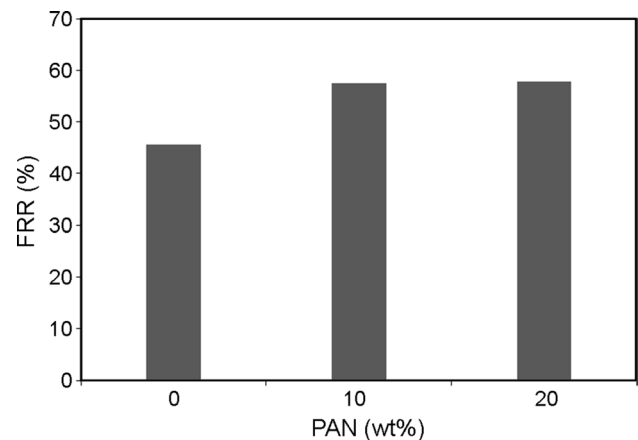


Fig. 6 FRR of PVC/PAN blend membranes

reported, which may be attributed to the higher hydrophilicity [38] or amplified turbulence near the membrane surface [40].

Effect of PAN on mechanical and thermal properties of membranes

The tensile strength of pure PVC membrane dropped (decline in break stress) by adding PAN to PVC (Table 3). This can be attributed to the change in the membrane structure caused by adding PAN to PVC. Macrovoids and porous walls observed in the cross section lead to a reduction in the strength of the membrane [41]. In particular, the high incompatibility of the blend components resulted in a remarkable deterioration of the membrane strength. On the other hand, the membrane elongation was enhanced by adding PAN to the PVC perhaps, due to an increase in the membrane flexibility. This flexibility might be due to the high incompatibility of PVC and PAN, which tends to lower T_g of the PVC amorphous phase compared to pure PVC [14, 42]. Therefore, higher elongation-at-break was obtained along with lower tensile strength [42], which was more pronounced when the PAN content was increased.

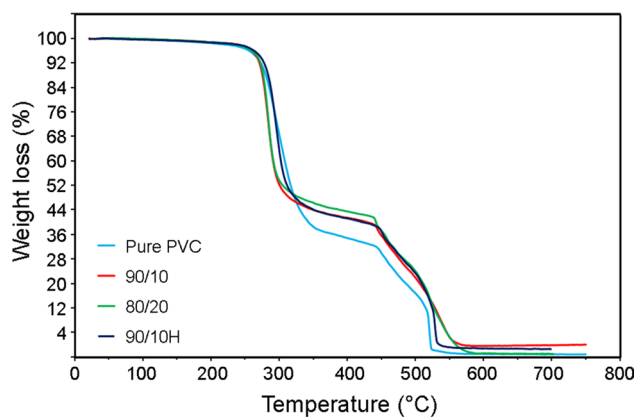


Fig. 7 TG curves of PVC/PAN blend membranes (pure PVC, 90/10, 80/20) and PVC/PAN blend membrane hydrolyzed (90/10H) with 0.5 mol/L NaOH for 0.5 h

Figure 7 shows the results of TGA for PVC and its blend membranes. As can be seen, a substantial weight loss (~ 60%) occurs in the temperature range of 270 to 310 °C, where the PVC polymer chains are degraded thermally. The material was carbonized over 450 °C [43]. Significant thermal degradations for the pure PVC, PVC/PAN (90/10), and PVC/PAN (80/20) blend membranes are started at 302, 285, and 284 °C, respectively. As reported in the literature, PAN thermal degradation starts at a lower temperature compared to PVC [44]. Hence, it can be inferred that the thermal stability of the pure PVC membrane is decreased with the addition of PAN to PVC. However, the blend membranes display lower weight loss (between 300 and 450 °C) compared to pure PVC.

Structure of modified membranes

As discussed previously, the PVC/PAN (90/10) blend membrane was subjected to hydrolysis in the NaOH alkaline solution to modify its performance. The hydrolysis reaction was provoked at three concentrations and modification times owing to the importance of the effect of these variables on the final membrane properties. Since the cross section of 80/20 (PVC/PAN) blend membrane was irregular, the 90/10 (PVC/PAN) blend membrane was chosen for the modification process. Figure 8 displays the FTIR spectra of the unmodified membrane and hydrolyzed membrane at three concentrations (0.5, 1, and 1.5 mol/L) and three modification times (0.5, 1, and 1.5 h). As shown in the spectrum of the unmodified membrane, the peaks at 2243 and 1736 /cm are due to the stretching vibration of nitrile (–CN) and carbonyl (–C=O) groups in acrylonitrile and vinyl acetate monomers, respectively [21, 45, 46]. A new peak (at 1561 /cm) is created by hydrolysis in the spectra of the membranes, which is due to stretching vibration of –C=O present at the

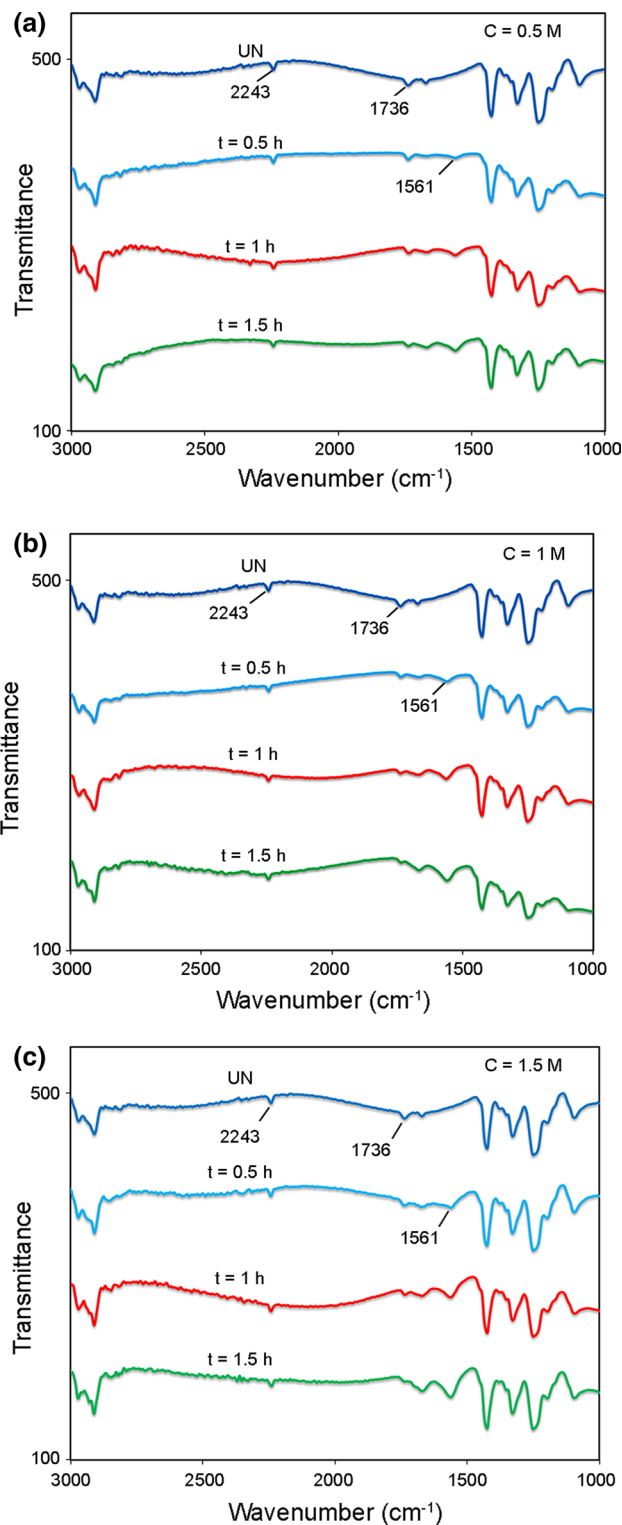


Fig. 8 FTIR spectra of PVC/PAN (90/10) blend membranes, unmodified membrane (UN), and membrane hydrolyzed at three concentrations and times ($C = 0.5, 1$ and 1.5 M and $t = 0.5, 1$ and 1.5 h)

carboxyl or amide groups [45]. This peak grows in intensity by increasing the hydrolysis concentration (at a given constant time) and the hydrolysis time (at a given constant concentration). The highest intensity of this peak is observed at a concentration of 1.5 mol/L and modification time of 1.5 h. The intensity of 1736 /cm peak declines by hydrolysis which could be due to the hydrolysis of acetate groups present in vinyl acetate monomer. Since the characteristic peak of nitrile groups (2243 /cm) did not change remarkably, it could be concluded that only some of the $-\text{CN}$ groups were hydrolyzed in contact with the NaOH solution.

Contact angle and pure water flux of hydrolyzed membranes

The contact angle and pure water flux of hydrolyzed membranes at modification times of 0.5, 1, and 1.5 h and concentrations of 0.5, 1, and 1.5 mol/L are shown in Figs. 9 and 10. As can be seen, the contact angle of membrane is reduced as a result of hydrolysis. This decrease is attributed to the formation of hydrophilic groups such as carboxyl or amide by hydrolysis, as illustrated in the previous section. The contact angle of membranes is reduced with an increase in modification concentration and time. The lowest contact angle ($44 \pm 0.9^\circ$) belongs to the membrane hydrolyzed at NaOH concentration of 1.5 mol/L and modification time of 1.5 h. This could be explained in terms of increased degree of hydrolysis at higher concentrations of NaOH and longer contact times.

Furthermore, the pure water flux of membrane (Fig. 10) increases by hydrolysis at concentration of 0.5 mol/L and modification time of 0.5 h, from $53.5 \pm 5.1 \text{ L/m}^2 \text{ h}$ (for unmodified membrane) to $75.6 \pm 7.2 \text{ L/m}^2 \text{ h}$, which is mainly due to increment of membrane hydrophilicity (i.e., decline in contact angle from $67.5^\circ \pm 1.9^\circ$ to $65^\circ \pm 1.1^\circ$). However, the membrane pure water flux drops with an

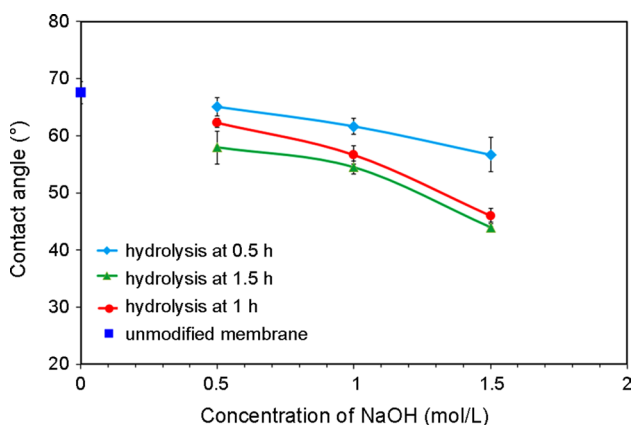


Fig. 9 Contact angle of PVC/PAN (90/10) blend membrane hydrolyzed at modification times of 0.5, 1, and 1.5 h

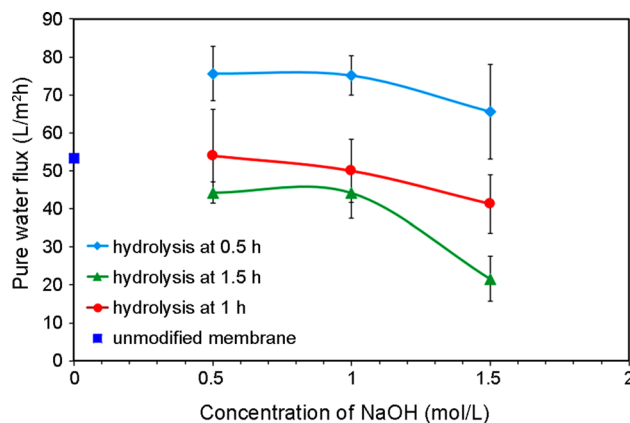


Fig. 10 Pure water flux of PVC/PAN (90/10) blend membrane hydrolyzed at modification times of 0.5, 1, and 1.5 h

increase in the modification concentration and time despite increased membrane hydrophilicity. The lowest membrane pure water flux ($21.6 \pm 5.9 \text{ L/m}^2 \text{ h}$) is obtained by hydrolysis at the concentration of 1.5 mol/L and the modification time of 1.5 h. Since hydrolysis affects both hydrophilicity and pore size of the membrane surface, increased hydrolysis concentration and time can reduce the pore size and subsequently the pure water flux. During hydrolysis with alkaline solutions, the swelling of unstable chains occurs due to the repulsive interactions between the chains carrying COO^- ions and adsorbed water. Carboxyl functional groups in the form of $\text{COO}^- \text{Na}^+$ create a pure negative charge on the membrane surface. These groups cause repulsive interactions between unstable chains, and the chains swell on the pores of membrane surface and hence reduce the pore size and pure water flux [20]. Moreover, the pure water flux of hydrolyzed membrane at the concentration of 0.5 mol/L and the modification time of 1 h shows a minor change (from 53.5 ± 5.1 to $53.9 \pm 12.3 \text{ L/m}^2 \text{ h}$) compared to that of unmodified membrane, suggesting that increased hydrophilicity and reduced pore size balance the effect of each other somewhat. Nevertheless, it seems that the pore size reduction dominates hydrophilicity with further increase of hydrolysis concentration or contact time.

Effect of hydrolysis on membrane morphology

To study the effect of hydrolysis concentration and time on membrane morphology, SEM images were taken from the membranes hydrolyzed at a constant concentration of 0.5 mol/L with different modification times of 0.5, 1, and 1.5 h, and constant time of 1.5 h at 0.5, 1, and 1.5 mol/L concentrations (Fig. 11). As can be observed, the cross section of the membranes hydrolyzed at the concentration of 0.5 mol/L and the modification times of 0.5 and 1 h (Fig. 11a, b) have not changed significantly compared to

the cross section of unmodified membrane (Fig. 5e). These results reveal that the hydrophilicity resulted from hydrolysis has been dominant in the morphological changes occurred at the concentration of 0.5 mol/L and the hydrolysis times of 0.5 and 1 h. As a result, compared to pure water flux of the unmodified membrane, the pure water flux increased under this hydrolysis condition, as demonstrated in the previous section.

However, as shown in Fig. 11c, the number and size of finger-like pores dropped with an increase in modification time from 0.5 to 1.5 h, indicating morphological changes at higher modification times. It takes time for PAN molecules

to move to change the morphology. Thus, at short modification times, when the chemical conversion from $-CN$ to COO^-Na^+ is relatively fast, the membrane surface becomes hydrophilic, but the morphological changes remain negligible [27].

Pore walls grow thicker by increasing the hydrolysis concentration from 0.5 to 1 mol/L at constant modification time of 1.5 h (Fig. 11d). As shown in Fig. 11e, the finger-like pores almost disappear with the emergence of smaller pores caused by the increase in NaOH concentration from 1 to 1.5 mol/L. As modification concentration and time are increased to 1.5 mol/L and 1.5 h, respectively, pore walls

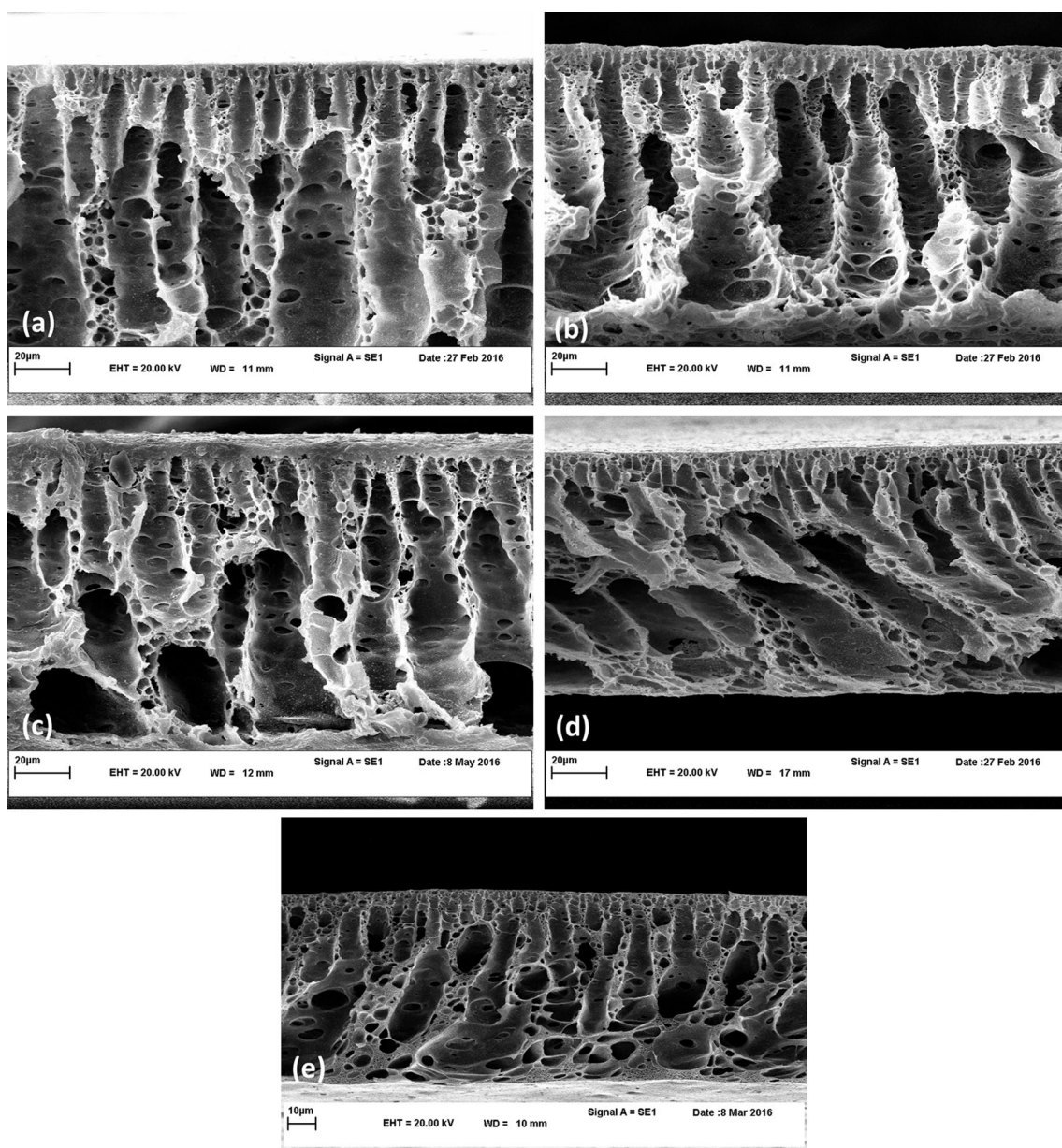


Fig. 11 SEM micrographs of cross section of membranes hydrolyzed at different modification times and concentrations **a** 0.5 h and 0.5 mol/L; **b** 1 h and 0.5 mol/L; **c** 1.5 h and 0.5 mol/L; **d** 1.5 h and 1 mol/L; and **e** 1.5 h and 1.5 mol/L

are covered with a thicker layer of the swollen polymer, and hence, the pore size decreases, leading to reduction of the membrane pure water flux.

Comparison of rejection, fouling resistance, and surface roughness of PVC/PAN (90/10) blend membrane before and after hydrolysis

The membrane pure water flux was the highest for the PVC/PAN (90/10) blend membrane hydrolyzed at the concentration of 0.5 mol/L and the modification time of 0.5 h. Therefore, the rejection, fouling resistance, and surface roughness were investigated for this membrane to draw a comparison with the unmodified membrane. According to Table 3, the FRR value increases from 57.6 to 71.6% by hydrolysis under aforementioned conditions as a result of increase in the hydrophilicity of the membrane. Furthermore, the BSA rejection of hydrolyzed membrane is 92.4 ± 3.8 , which does not show a significant change compared to the rejection value of unmodified membrane (94 ± 0.7). The reduction in the BSA rejection for the membrane hydrolyzed at the concentration of 0.5 mol/L for 0.5 h could be due to the hydrophilicity due to hydrolysis, which was dominant for morphological changes under these conditions. Lohokare et al. [20] also reported a lower BSA rejection for hydrolyzed PAN membranes, which was due to higher surface hydrophilicity rather than morphological changes.

The RMS roughness of hydrolyzed PVC/PAN (90/10) blend membrane was higher than that of the unmodified one (Table 3). This could be due to the change of some functional groups on the membrane surface upon alkali treatment. As mentioned in the previous section (the structure of modified membranes), the $-\text{CN}$ groups in PAN could be converted to the carboxyl or amide groups during hydrolysis reaction. Parashuram et al. [47] also showed a similar increase in surface roughness for poly(acrylonitrile-*co*-methacrylic acid) hollow fiber membrane upon treatment with aqueous NaOH solutions at varying concentrations.

Mechanical and thermal properties of PVC/PAN (90/10) blend membrane before and after hydrolysis

The mechanical properties of the unmodified and hydrolyzed membranes are listed in Table 3. As can be seen, the hydrolyzed membrane demonstrates improved mechanical properties compared to the unmodified one. Hence, the break stress and elongation of the membrane increased from 1.9 to 2.6 MPa and from 45.3 to 52.2%, respectively. Before the hydrolysis, due to the lack of miscibility, the resultant weak interfaces between PVC and PAN act as stress concentration points. However, as shown by FTIR analysis, during hydrolysis reaction, some of the

nitrile groups present in PAN could be converted into the carboxyl or amide groups. As a small number of these groups situated on the pore walls are sufficient to interact with PVC [13], it seems that the membrane integrity under stress is slightly improved, and therefore, enhanced mechanical properties are observed.

The TGA thermograms also exhibited improved thermal stability after hydrolysis (Fig. 7). Furthermore, a significant thermal degradation for the hydrolyzed PVC/PAN (90/10) blend membrane was started at 295 °C, which was higher than the onset degradation temperature of the unmodified membrane (285 °C). Therefore, it can be concluded that the thermal stability of PVC/PAN (90/10) blend membrane was increased by hydrolyzing the membrane in 0.5 mol/L NaOH solution for 0.5 h. As described above, it appears that the higher thermal stability of the membrane could be attributed to the enhancement of the PVC–PAN interactions induced by hydrolysis reaction.

Conclusion

In this work, polyacrylonitrile (PAN) was used as a second polymer to modify polyvinylchloride (PVC) membranes. The miscibility of PVC/PAN blend was investigated using a simple thermodynamic theory based on the compressible regular solution (CRS) model, which for evaluation of miscibility only requires the properties of blend components. The results showed that the PVC/PAN blend was immiscible for all compositions in the temperature range of -25 to 225 °C. However, according to the dilute solution viscometry (DSV) method, both two polymers showed some compatibility for PAN contents greater than 20 wt%. The pure water flux of the PVC membrane increased by about 41 and 76% by adding 10 and 20 wt% PAN, respectively. This increased membrane flux could be attributed to both increased hydrophilicity and immiscibility of PAN/PVC blend, which resulted in polymer–polymer phase separation and interfacial microvoid formation. Moreover, the hydrolysis of the 90/10 (PVC/PAN) blend membrane was performed in sodium hydroxide solution at a temperature of 70 °C, concentrations of 0.5, 1, and 1.5 mol/L and modification times of 0.5, 1, and 1.5 h. The results showed that the pure water flux of the membrane was increased by about 42% after hydrolysis in the presence of a 0.5 mol/L solution of NaOH with a modification time of 0.5 h due to increased membrane hydrophilicity. This modification also led to enhanced mechanical and thermal performance as well as higher FRR compared to those of unmodified membranes.

References

- Gholami A, Moghadassi AR, Hosseini SM, Shabani S, Gholami F (2013) Preparation and characterization of polyvinyl chloride based nanocomposite nanofiltration-membrane modified by iron oxide nanoparticles for lead removal from water. *J Ind Eng Chem* 20:1517–1522
- Hosseini SM, Madaeni SS, Zendehnam A, Moghadassi AR, Khodabakhshi AR, Sanaeepur H (2013) Preparation and characterization of PVC based heterogeneous ion exchange membrane coated with Ag nanoparticles by (thermal-plasma) treatment assisted surface modification. *J Ind Eng Chem* 19:854–862
- Behboudi A, Jafarzadeh Y, Yegani R (2016) Preparation and characterization of TiO₂ embedded PVC ultrafiltration membranes. *Chem Eng Res Des* 114:96–107
- Demirel E, Zhang B, Papakyriakou M, Xia S, Chen Y (2017) Fe₂O₃ nanocomposite PVC membrane with enhanced properties and separation performance. *J Membr Sci* 529:170–184
- Vladkova TG, Dineff P, Stojcheva R, Tomerova B (2003) Ion-plasma modification of polyvinylchloride microfiltration membranes. *J Appl Polym Sci* 90:2433–2440
- Sun PB, Sun B (2003) Effect of compatibility of PVC/P2 alloy system on membrane structure and performance. *Ann NY Acad Sci* 984:267–278
- Peng Y, Sui Y (2006) Compatibility research on PVC/PVB blended membranes. *Desalination* 196:13–21
- Liu J, Su Y, Peng J, Zhao X, Zhang Y, Dong Y, Jiang ZH (2012) Preparation and performance of antifouling pvc/cpvc blend ultrafiltration membranes. *Ind Eng Chem* 51:8308–8314
- Fan X, Su Y, Zhao X, Li Y, Zhang R, Zhao J, Jiang Zh, Zhu J, Ma Y, Liu Y (2014) Fabrication of polyvinyl chloride ultrafiltration membranes with stable antifouling property by exploring the pore formation and surface modification capabilities of polyvinyl formal. *J Membr Sci* 464:100–109
- Babu PR, Gaikar VG (2000) Preparation, structure, and transport properties of ultrafiltration membranes of poly(vinyl chloride) and poly(vinyl pyrrolidone) blends. *J Appl Polym Sci* 77:2606–2620
- Davood Abadi Farahani MH, Rabiee H, Vatanpour V, Borghei SM (2016) Fouling reduction of emulsion polyvinylchloride ultrafiltration membranes blended by PEG: the effect of additive concentration and coagulation bath temperature. *Desalin Water Treat* 57:1–14
- Liu WD, Zhang YH, Fang LF, Zhu BK, Zhu LP (2012) Antifouling properties of poly(vinyl chloride) membranes modified by amphiphilic copolymers P(MMA-B-MAA). *Polym Sci* 30:568–577
- Babu PR, Gaikar VG (1999) Preparation, structure, and transport properties of ultrafiltration membranes of poly(vinyl chloride) (PVC), carboxylated poly(vinyl chloride) (CPVC), and PVC/CPVC blends. *J Appl Polym Sci* 73:1117–1130
- Gu A (2001) Study of ultrafiltration membrane made from polyvinyl chloride/polyacrylonitrile blend. *Polym Plast Technol Eng* 40:615–625
- Mei S, Xiao C, Hu X (2012) Interfacial microvoid formation of poly(vinyl chloride)/polyacrylonitrile blend hollow-fiber membranes. *J Appl Polym Sci* 124:E9–E16
- Rabiee H, Seyedi SM, Rabiee H, Alvandifar N, Arya A (2017) Preparation and characterization of PVC/PAN blend ultrafiltration membranes: effect of PAN concentration and PEG with different molecular weight. *Desalin Water Treat* 58:1–11
- Pacharasakoolchai S, Chinpa W (2014) Improved permeation performance and fouling-resistance of Poly(vinyl chloride)/Polycarbonate blend membrane with added Pluronic F127. *Songklanakarin J Sci Technol* 36:209–215
- Wu MM (2001) Acrylonitrile and acrylonitrile polymers. *Encyclopedia of Polymer Science and Technology*. Wiley, New Jersey
- Scharnagl N, Buschatz H (2001) Polyacrylonitrile (PAN) membranes for ultra and microfiltration. *Desalination* 139:191–198
- Lohokare HR, Kumbharkar SC, Bhole YS, Kharul UK (2006) Surface modification of polyacrylonitrile based ultrafiltration membrane. *J Appl Polym Sci* 101:4378–4385
- Zhang X, Xiao C, Hu X (2013) Preparation and properties of polysulfone/polyacrylonitrile blend membrane and its modification with hydrolysis. *Desalin Water Treat* 51:3979–3987
- Amirilargani M, Sabetghadam A, Mohammadi T (2012) Polyethersulfone/polyacrylonitrile blend ultrafiltration membranes with different molecular weight of polyethylene glycol: preparation, morphology and antifouling properties. *Polym Adv Technol* 23:398–407
- Wang ZG, Wan LS, Xu ZK (2007) Surface engineering of polyacrylonitrile-based asymmetric membranes towards biomedical applications: an overview. *J Membr Sci* 304:8–23
- Reddy AVR, Patel HR (2008) Chemically treated polyethersulfone/polyacrylonitrile blend ultrafiltration membranes for better fouling resistance. *Desalination* 221:318–323
- Mei S, Xiao C, Hu X, Shu W (2011) Hydrolysis modification of PVC/PAN/SiO₂ composite hollow fiber membrane. *Desalination* 280:378–383
- Kim IC, Yun HG, Lee KH (2002) Preparation of asymmetric polyacrylonitrile membrane with small pore size by phase inversion and post-treatment process. *J Membr Sci* 199:75–84
- Oh NW, Jegal J, Lee KH (2001) Preparation and characterization of nanofiltration composite membranes using polyacrylonitrile (PAN). I. Preparation and modification of PAN supports. *J Appl Polym Sci* 80:1854–1862
- An QF, Qian WJ, Sun HB, Wang LN, Zhang L, Chen HL (2003) Compatibility of PVC/EVA blends and the pervaporation of their blend membranes for benzene/cyclohexane mixtures. *J Membr Sci* 222:113–122
- Mathew M, Ninan KN, Thomas S (1998) Compatibility studies of polymer–polymer systems by viscometric techniques: nitrile-rubber-based polymer blends. *Polymer* 39:6235–6241
- Ruzette AVG, Mayes AM (2001) A simple free energy model for weakly interacting polymer blends. *Macromolecules* 34:1894–1907
- Robeson LM (2007) *Polymer blends: a comprehensive review*. Carl Hanser Verlag GmbH & Co. KG, Munich
- Walsh D, Paul Z (1995) *Standard pressure volume temperature data for polymers*. CRC Press, Pennsylvania
- Bernal-García JM, Guzmán-López A, Cabrales-Torres A, Estrada-Baltazar A, Iglesias-Silva GA (2008) Densities and viscosities of (*N,N*-dimethylformamide + water) at atmospheric pressure from (283.15 to 353.15) K. *J Chem Eng Data* 53:1024–1027
- Mark JE (2007) *Physical properties of polymers handbook solubility parameters*. Springer, New York
- Barzin J, Sadatnia B (2007) Theoretical phase diagram calculation and membrane morphology evaluation for water/solvent/polyethersulfone systems. *Polymer* 48:1620–1631
- Pospiech D, Gottwald A, Jehnichen D, Friedel P, John A, Harnisch C, Voigt D, Khimich G, Bilibin AY (2002) Determination of interaction parameters of block copolymers containing aromatic polyesters from solubility parameters obtained from solution viscosities. *Colloid Polym Sci* 280:1027–1037
- Fashandi H, Karimi M (2014) Influence of solvent/polymer interaction on miscibility of PMMA/PCL blend: thermal analysis approach. *J Text Polym* 2:71–78

38. Panda SR, De S (2015) Preparation, characterization and antifouling properties of polyacrylonitrile/polyurethane blend membranes for water purification. *RSC Adv* 5:23599–23612
39. Jiang S, Wang J, Wu J, Chen Y (2015) Poly(vinyl chloride) and poly(ether sulfone)-*g*-poly(ether glycol) methyl ether methacrylate blend membranes with improved ultrafiltration performance and fouling resistance. *J Appl Polym Sci* 132:1–10
40. Moghimifar V, Esmaili Livari A, Raisi A, Aroujalian A (2015) Enhancing the antifouling property of polyethersulfone ultrafiltration membranes using NaX zeolite and titanium oxide nanoparticles. *RSC Adv* 5:55964–55976
41. Chinpa W (2008) Preparation and characterization of an asymmetric porous poly(vinyl chloride)/poly(methyl methacrylate-*co*-methacrylic acid) membrane. *Sci Asia* 34:385–389
42. Alsahy QF (2012) Hollow fiber ultrafiltration membranes prepared from blends of poly(vinyl chloride) and polystyrene. *Desalination* 294:44–52
43. Mohagheghian M, Sadeghi M, Pourafshari Chenar M, Naghsh M (2014) Gas separation properties of polyvinylchloride (PVC)-silica nanocomposite membrane. *Korean J Chem Eng* 31:2041–2050
44. Czegeny Z, Jakab E, Blazsó M (2002) Thermal decomposition of polymer mixtures containing poly(vinyl chloride). *Macromol Mater Eng* 287:277–284
45. Wang J, Yue Z, Ince JS, Economy J (2006) Preparation of nano-filtration membranes from polyacrylonitrile ultrafiltration membranes. *J Membr Sci* 286:333–341
46. Cetiner S, Sen S, Sarac AS (2013) Acrylonitrile/vinyl acetate copolymer nanofibers with different vinylacetate content. *J Appl Polym Sci* 127:3830–3838
47. Parashuram K, Maurya SK, Rana HH, Singh PS, Ray P, Reddy AVR (2013) Tailoring the molecular weight cut off values of polyacrylonitrile based hollow fibre ultrafiltration membranes with improved fouling resistance by chemical modification. *J Membr Sci* 425–426:251–261